Scaled structures in late stages of microphase separation of binary paraffin mixtures

Peng Wei Zhu and J. W. White
Research School of Chemistry, The Australian National University, Canberra, ACT 2601, Australia

J. E. Epperson
Materials Science Division, Argonne National Laboratory, Argonne, Illinois 60439

(Received 10 July 2000)

Since the dynamic properties in paraffin mixtures are different from those in alloys and polymer blends, paraffin mixtures are believed to be another class of substances establishing the ''universality'' of the dynamical scaling behavior of phase separation. In this paper, the scaled structures of microphase separation in paraffin mixtures are described using a scaling function based on a two-phase model with kinetics based on the Cahn-Hilliard equation. It has been demonstrated that at the late stages of the microphase separation the scaling behavior in the paraffin mixtures agrees well with the universal features predicted by the scaling function. The scaled structures of microphase separation in paraffin mixtures can be directly calculated from the volume fraction of the minority phase without any adjustable parameter.

PACS number(s): 64.70.−p, 64.75.+g, 78.70.Nx

I. INTRODUCTION

The kinetics of phase separation in mixtures have attracted much attention [1–4]. Phase separation of mixtures on quenching starts from a homogeneous state and proceeds through a series of heterogeneous states, as is the case with the liquid-gas phase transition in one-component systems or with liquid-liquid and solid-solid phase separation in two-component systems. Such phenomena include nucleation, spinodal decomposition, coarsening, and Ostwald ripening. The kinetic processes can generally be divided into two main stages, depending on the degree of time evolution. In the early stages (including the nucleation and growth regime), there are dominant concentration fluctuations in a homogeneous phase, which lead to the creation of new phases. In the late stages, neither nucleation of new phases nor variation in composition occurs, and the gradual aggregation of new phases occurs. Finally, the entire system settles down to a macroscopic two-phase state. The kinetics of phase separation have been extensively studied in many systems, including binary alloys, binary fluids, polymer blends, glasses, ferroelectric crystals, and magnetic materials [1–4]. The dynamical scaling behavior of late stages of phase separation has been a focus of interest.

The dynamic scaling of phase separation indicates that the late stages of phase separation are entirely controlled by a unique characteristic length $\xi(t)$. A phase-separating system with scaling characteristics is considered to have a self-similar structure. At the experimental level, determination of whether or not the x-ray or neutron scattering function or structure factor $S(Q,t)$ exhibits a dynamic scaling is an important test. A direct consequence of the dynamic scaling is that the structure function follows a simple asymptotic behavior at late stages of phase separation. Conservation laws are known to be an important factor in governing the behavior of late stage kinetics. In practice, moments of the structure factor Q_n, the momentum transfer Q_m corresponding to the maximum value of the structure factor, or the radius of gyration R_g can be chosen as a unique characteristic length. Dynamic scaling has been found in many different mixtures and appears to be universal [1–4].

Normal paraffin mixtures with different chain lengths are among the simplest anisotropic molecular systems. A study of microphase separation in paraffin mixtures is interesting because this system forms a bridge between conventional substances and macromolecules. It is known that when the difference in carbon number of a binary paraffin mixture exceeds a certain value, a microphase is formed in a period of days at room temperature after slowly cooling or quick quenching from the melt [5–9]. The microphase separation in paraffin mixtures takes place in a highly crystalline, anisotropic solid and involves chain conformational ordering. What is more, it has been found that the process of microphase separation in some binary paraffin mixtures is always accompanied by precipitation of some almost pure paraffin crystals [7–9]. Apparently, the microphase separation in paraffin mixtures has behavior not found in other systems like alloys and polymer blends. For example, there is no so-called conformational ordering in alloys, while the phase separation in polymer blends very likely occurs in an amorphous condition on quenching from the melt. Since the properties and structures of paraffin mixtures are different from those of alloys and polymer blends, paraffin mixtures are believed to be another class of substances establishing the ''universality'' of the scaling behavior associated with phase separation.

We have studied the kinetics of microphase separation in binary paraffin mixtures $C_{30}H_{62}/C_{36}D_{74}$ and $C_{30}D_{62}/C_{36}H_{74}$, using small-angle neutron scattering (SANS) [7–9]. The deuteration provides an isotopic contrast of the mixtures for SANS experiments. Since the volume of a deuterated paraffin is different from that of its hydrogenous version, the deuteration alters the volume difference between the two components. Note that the main driving force for the microphase separation in a binary paraffin mixture is the volume difference [5–9]. SANS data were taken from a number of compositions and several temperatures inside the phase separation regions. In addition to the temperature and composition,

vacancies and lamellar boundaries are believed to influence the kinetics of microphase separation in paraffin mixtures. Two dynamic scaling functions were introduced to analyze the late stages of microphase separation in the $C_{30}H_{62}/C_{36}D_{74}$ and $C_{30}D_{62}/C_{36}H_{74}$ mixtures [9]. These scaling functions were proposed by Marro, Lebowitz, and Kalos (MLK) [10] and by Phani *et al.* (PLKP) [11]. Both MLK and PLKP scaling models were obtained from computer simulations and appear to be a universal feature of late stages of coarsening kinetics. The late stages of microphase separation in the C_{30}/C_{36} mixtures agree well with the theoretical predictions of MLK and PLKP scaling functions [9].

It is worth noting that the MLK and PLKP methods do not clearly give a composition dependence of the scaling function. It has been found from experiments [12–14] and computer simulations [15–17], however, that the morphology of a phase-separating system depends on the composition. Structural patterns of a phase-separating system at smaller volume fractions of the minority phase are considered to be isolated clusters, whereas an interconnected structure is obtained at higher volume fractions of the minority phase.

Fratzl and Lebowitz (FL) have presented a scaling function in terms of a two-phase model [18]. The physical picture of the two-phase model is that at late stages of phase separation a system consists of two large domains which are partially separated by a thin interface region. A theoretical interpretation of the FL scaling function was further given [19] both on the basis of asymptotic analysis [20] of the Cahn-Hilliard equation [21] and on the hypothesis of asymptotic self-similarity. The FL scaling function has been successfully tested for many different systems [18], including solid alloys, polymer blends, liquid mixtures, and theoretical models (such as Ising and Ginzburg-Landau models) used in computer simulations. The purpose of this paper is to perform a quantitative test of the universality of the FL scaling function for the late stages of microphase separation in paraffin mixtures.

II. EXPERIMENTAL DETAILS

$C_{30}H_{62}$ and $C_{36}H_{74}$ were obtained from Supelco (Bellefonte, PA) and the corresponding deuterated analogs, $C_{30}D_{62}$ and $C_{36}D_{74}$ were from MDS Isotopes (Montreal, Quebec, Canada). They had purity grades greater than 99.5%. The deuterated samples had a manufacturer's specification indicating a deuterium concentration greater than 99.0%. $C_{30}H_{62}/C_{36}D_{74}$ and $C_{30}D_{62}/C_{36}H_{74}$ (C_{30}/C_{36}) mixtures, on a mole/mole basis, were made from the crystalline hydrocarbons, which were melted together in an inert atmosphere in the same silica ultraviolet absorption spectroscopy cells (1 mm thick) used for the subsequent neutron scattering experiments. The C_{30}/C_{36} mixtures were left to interdiffuse for a period of 1–2 days in the melt before quenching. Quenched $C_{30}H_{62}/C_{36}D_{74}$ mixtures with mole ratios 4:1, 1:1, 3:8, 1:4, and 1:9 were made by dipping the cells into water at 27 °C. The 1:4 $C_{30}H_{62}/C_{36}D_{74}$ mixture was also quenched to 26, 30, 33, and 41 °C. The $C_{30}D_{62}/C_{36}H_{74}$ mixture was quenched to 20 °C. The experimental phase diagram of binary C_{30}/C_{36} mixtures has been determined by Snyder *et al.* [22]. At the compositions and temperatures used the processes observed in the scattering should fall inside the microphase separation region of the phase diagram.

The small-angle diffractometer (SAD) at the Intense Pulsed Neutron Source (IPNS), Argonne National Laboratory, was used for the neutron scattering measurements. The small-angle scattering of neutrons was detected using time-of-flight (TOF) analysis and wavelengths were in the range $2<\lambda<14$ Å. Scattering data from the different wavelengths were appropriately ''binned'' as a function of the momentum transfer $Q=4\pi\sin(\theta/\lambda)$, where θ is the half scattering angle. This not only allows the scattering function to be determined over a wide range of the momentum transfer but also provides sufficient intensity for the patterns to be measured in relatively short time intervals. The other advantage of this instrument for the present work is that, by binning different wavelength intervals in the time-of-flight spectrum, the scattering intensity can be generated using only particular wavelength bands. This allows the wavelength dependence of the scattering function to be determined and hence checks made for multiple scattering and refraction. The neutron scattering data were reduced using the standard program REDUCE and normalized using a standard scatterer to absolute intensities (cm^{-1}). Scattering patterns from quenched samples were recorded at 1 h intervals after quenching to observe the growth of microphase separation in scattering patterns. Runs of up to 14 h were used depending upon the kinetics. Any scattering function was thus the mean scattering during the 1 h period of observation.

III. RESULTS AND DISCUSSION

Figure 1 representatively shows the time evolution of the SANS intensity of the $C_{30}H_{62}/C_{36}D_{74}$ mixtures at 27 °C after the initial quench from the melt. The scattered intensity was plotted as IQ^2 vs Q. Details of the temperature and composition dependence of SANS patterns have been reported [7–9]. Since the first scattering patterns were collected at a mean time of 30 min after quenching, the results observed represent intermediate and later times of the microphase separation in the C_{30}/C_{36} mixtures.

In the present work, the first moment of the structure factor $Q_1(t)$ was introduced as a measure of the characteristic length $\xi(t)$. Moments of the structure factor $S(Q,t)$ are defined as

$$Q_n(t)=\frac{\sum Q^n S(Q,t)}{\sum S(Q,t)}, \tag{1}$$

which is found to vary quite smoothly with time [23]. Quantitatively, the experimental criterion for the late stages can be obtained from the time independence of Q_2/Q_1^2. Plots of Q_2/Q_1^2 versus time were found to remain almost constant for different temperatures and compositions when the time was greater than about 270 min [9]. The FL scaling function was therefore tested within the time ranges determined from the

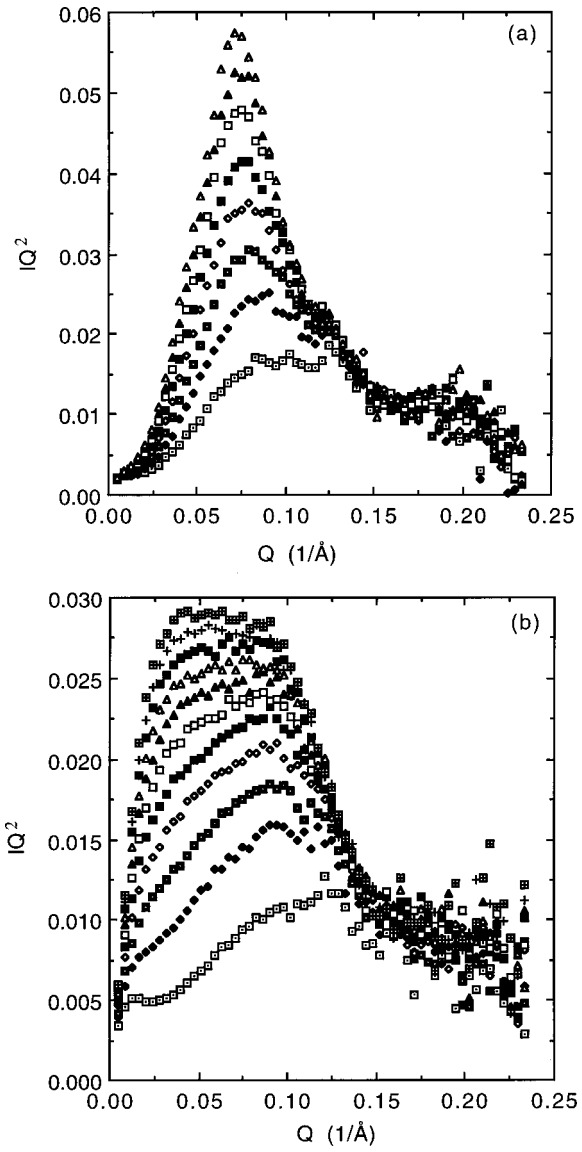

FIG. 1. The time evolution of IQ^2 versus Q for $C_{30}H_{62}/C_{36}D_{74}$ mixtures quickly quenched from the melt to 27 °C: (a) 1:1 and (b) 1:4. The first pattern was collected at a mean time of 30 min, and the increment was 60 min.

plots of Q_2/Q_1^2 versus time, although the scaling behavior was observed at much earlier times.

Phenomenological results and computer simulations suggest that the scaling function has the form [23–27]

$$S(Q,t)=J(t)F(Q\xi(t)) \tag{2}$$

where $F(Q\xi(t))$ is a time-independent scaling function of one variable and $J(t)$ is the scaling factor, which is proportional to ξ^{ν} in ν dimensions,

$$S(Q,t)\propto\xi(t)^{\nu}F(Q\xi(t)). \tag{3}$$

The structure factor $S(Q,t)$ can be directly measured by scattering techniques. There are various theories and simulations leading to different forms of $F(Q\xi(t))$. Fratzl and Lebowitz have constructed a normalized structure factor $L_{\nu}(x)$ as the scaling function $F(Q\xi(t))$ in the formula [18,19]

$$F(Q\xi(t))\propto L_{\nu}(x)=\frac{a_{\nu}x^4}{x^4+c_{\nu}}P_{\nu}(x), \tag{4}$$

where $x=Q/Q_1$ in the present work. In three dimensions, the scaling function $L_3(x)=L(x)$ has the simple analytical form [18,19]

$$P_3(x)=\frac{b_3}{b_3+(x^2-1+d_3)^2}, \tag{5}$$

$$b_3=\frac{4\gamma^2}{(1-\gamma^2)^2}(1-d_3), \tag{6}$$

$$c_3=\frac{d_3}{b_3-d_3(1-d_3)}, \tag{7}$$

$$a_3=(1+c_3)(1+d_3^2/b_3). \tag{8}$$

There are two free parameters d_3 and γ in the FL scaling function $L_3(x)$. The function has its maximum value 1 at $x=1$. The scaling function $L_3(x)$ is proportional to x^{-4} as $x\to\infty$ and to x^4 as $x\to 0$. The dependence $F(x)\sim x^{-4}$ at large x is physically equivalent to Porod's law [28]. For a two-phase system, the validity of Porod's law indicates a sharp phase boundary. In three dimensions, a deviation from Porod's law is due to a diffuse phase boundary or the presence of thermal density fluctuations. The dimension of a diffuse phase boundary could involve surface fractals [29,30].

Since the parameter d_3 has been empirically found to be 0.06, irrespective of the system [18], the FL scaling function has only one free parameter γ for the fitting of experimental data. The important feature of the FL scaling function is that the parameter γ is physically proportional to the interphase surface per unit volume at a given volume fraction ϕ of the minority phase and could be a measure of the equilibrium morphology of a phase-separating system [8,19]. Accordingly, the FL scaling function is determined by only one parameter: the volume fraction ϕ of the minority phase. The ϕ dependence of the scaling function $F(x)$ has been interpreted as a consequence of the hypothesis that the asymptotically self-similar ensemble of the interface configuration is completely determined by the volume fraction [19].

Figure 2 shows representative plots of the scaling function $L_3(x)$ versus x at different values of γ for the 1:1 and 1:4 $C_{30}H_{62}/C_{36}D_{74}$ mixtures at 27 °C. It can be seen from Fig. 2 that the peak width of the scaling function decreases with decreasing γ. The peak value of $L_3(x)$ was observed only when the parameter γ was greater than a critical value that depends on the composition. Typical results are shown in Fig. 3. When the parameter γ is greater than the critical value, there are infinite choices of γ corresponding to $L_3(x)=1$ for a given composition. In order to test whether or not there is composition dependence of γ in the present system, a $L_3(x)$ value 0.998, which is marginally smaller than 1, was chosen as a criterion for all scaling tests. Clearly, $\gamma=0.3$ for the 1:1 $C_{30}H_{62}/C_{36}D_{74}$ mixture is smaller than $\gamma=0.7$ for the 1:4 $C_{30}H_{62}/C_{36}D_{74}$ mixture at $L_3(x)=0.998$. In other words, the peak width of the scaling function $L_3(x)$ of 1:1 $C_{30}H_{62}/C_{36}D_{74}$ is narrower than that of 1:4 $C_{30}H_{62}/C_{36}D_{74}$ when the function just reaches its maximum.

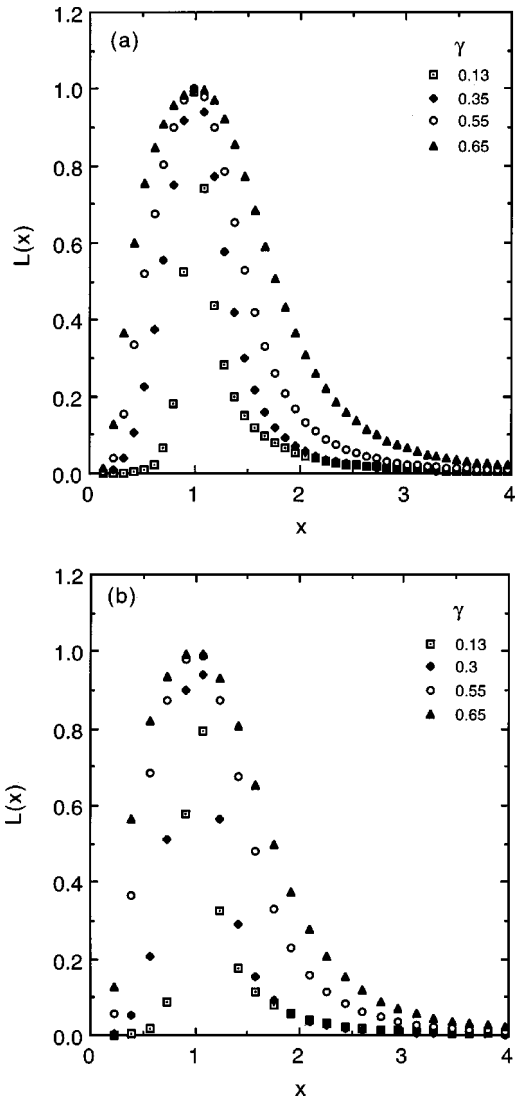

FIG. 2. Plots of the scaling function $L_3(x)$ versus $x=Q/Q_1$ at different values of γ for $C_{30}H_{62}/C_{36}D_{74}$ mixtures 630 min after quenching from the melt to 27 °C: (a) 1:1 and (b) 1:4.

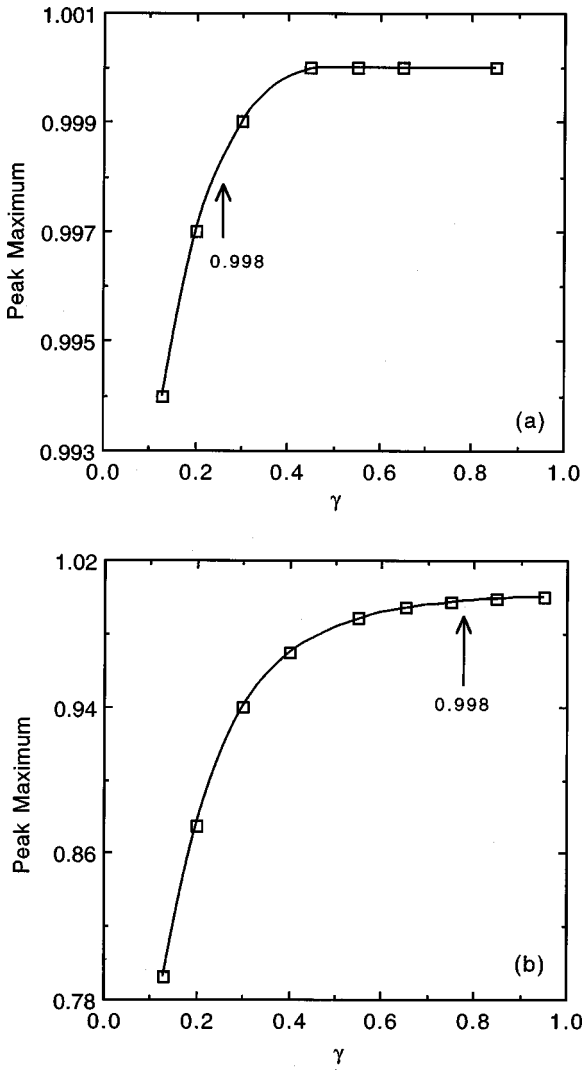

FIG. 3. Plots of the maximum value of $L_3(x)$ versus γ for $C_{30}H_{62}/C_{36}D_{74}$ mixtures 630 min after quenching from the melt to 27 °C: (a) 1:1 and (b) 1:4.

It is noted that $\gamma=0.3$ for the 1:1 mixture is comparable to the γ values for critical quenches at $\phi=0.5$ [18]. The composition dependence of the parameter γ predicted by the FL scaling function is demonstrated for the present system.

Figure 4 shows the scaling behavior of the experimental data of the 1:1 and 1:4 $C_{30}H_{62}/C_{36}D_{74}$ mixtures in terms of Eq. (4). As seen, the curves are scaled excellently together. The validity of the FL scaling function was well tested for all compositions of the $C_{30}H_{62}/C_{36}D_{74}$ mixtures in meaningful ranges of Eq. (4). The scaling behavior was also tested for a reverse pair, the 1:1 $C_{30}D_{62}/C_{36}H_{74}$ mixture. The results are shown in Fig. 5. Again, all curves at the different late times fall precisely on top of one another. Note that the γ value of the 1:1 $C_{30}D_{62}/C_{36}H_{74}$ mixture is 0.4 at $L_3(x)=0.998$, which is not much different from $\gamma=0.3$ of its reverse pair, 1:1 $C_{30}H_{62}/C_{36}D_{74}$.

Figure 6 shows the temperature dependence of the scaling function $L_3(x)$ of the 1:4 $C_{30}H_{62}/C_{36}D_{74}$ mixture. The parameter γ was chosen to be 0.65 since it was found to be almost independent of the quenching temperature at $L_3(x)=0.998$. As can be seen from Fig. 6, the scaling behavior is excellently obeyed at different temperatures. The same scaling behavior was observed for all compositions in the present study. These results are consistent with the prediction that the FL scaling function does not depend on the temperature for a given composition [18,19].

A representative $\log_{10}$-$\log_{10}$ plot of $L_3(x)$ versus x is shown in Fig. 7 for the 1:1 $C_{30}H_{62}/C_{36}D_{74}$ mixture at 26 °C. A slope of -4 was obtained at large x from the plot, indicating Porod's law as predicted by the FL scaling function. Porod's law at large x is obeyed for all compositions and temperatures in the present system. The observation of Porod's law indicates that the lamellar size of the paraffins becomes much larger than the thickness of the interfaces in the late stages of microphase separation. At small x, a slope of 4 was obtained from the $\log_{10}$-$\log_{10}$ plots. In terms of the domain growth of the Cahn-Hilliard equation [19], the dependence $L_3(x)\sim x^4$ at small x implies a local conservation of the order parameter and symmetry.

The morphology of a phase-separating system can be predicted from the FL scaling function [18,19]. A higher value of γ may be related to a morphology with spherical clusters of a minority component isolated in a matrix of a majority

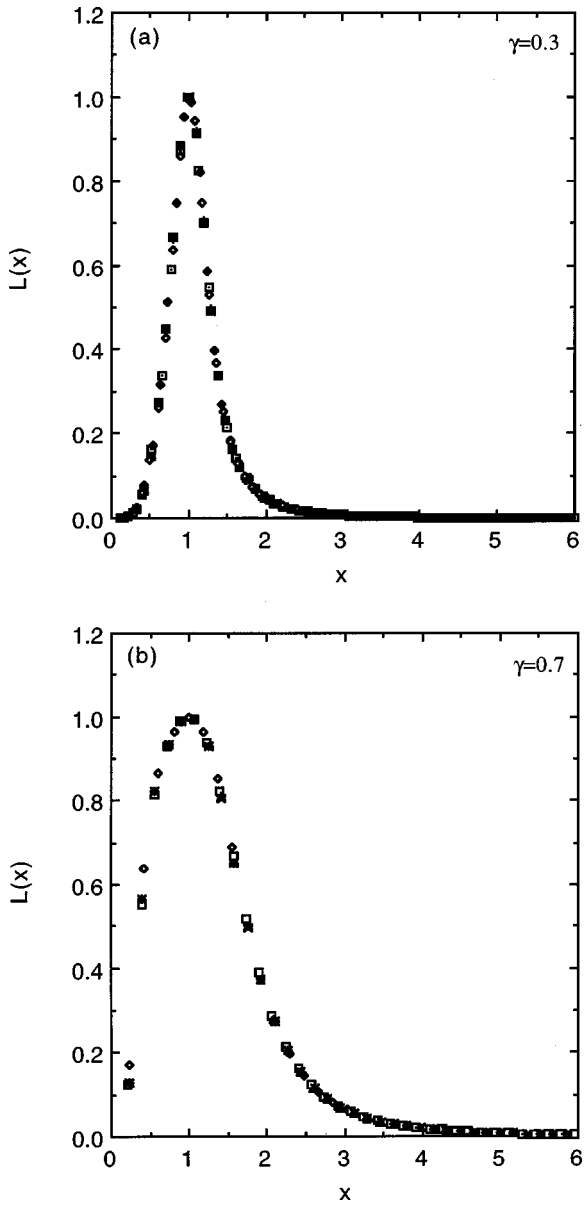

FIG. 4. Plots of the scaling function $L_3(x)$ versus $x=Q/Q_1$ for $C_{30}H_{62}/C_{36}D_{74}$ mixtures quickly quenched from the melt to 27 °C: (a) 1:1, $\gamma=0.3$ and (b) 1:4, $\gamma=0.7$. The first patterns were calculated at mean times of 330 and 270 min for 1:1 and 1:4, respectively, and the increment was 120 min.

component, whereas a lower value of γ could predict an interconnected morphology of rods or plates. Clusters of a minority component may not be completely spherical because of the anisotropy of the surface tension [19]. It is known that the morphology of the microphase in paraffin mixtures is a well-ordered lamellar structure [5–9]. In particular, the microphase of the 1:1 $C_{30}H_{62}/C_{36}D_{74}$ mixture is an alternation of lamellae of the two pure alkanes. If the terminologies used in the FL scaling function are introduced to the present system, the morphology of the microphase may be plausibly described as a platelike structure. The lower γ value of the 1:1 mixture corresponds to a highly interconnected morphology composed of alternative lamellae, whereas the higher γ value of the 4:1 or 1:9 $C_{30}H_{62}/C_{36}D_{74}$ mixture is associated with a morphology with lamellae of the minority components distributed randomly in

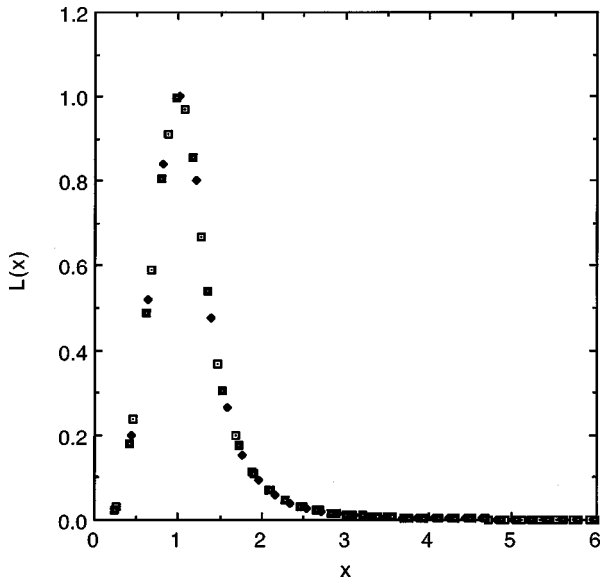

FIG. 5. Plots of the scaling function $L_3(x)$ versus $x=Q/Q_1$ at $\gamma=0.4$ for the 1:1 $C_{30}D_{62}/C_{36}H_{74}$ mixture quickly quenched from the melt to 20 °C. The first pattern was calculated at a mean time of 450 min, and the increment was 300 min.

the matrix of majority components.

The parameter γ is theoretically defined by [19]

$$\gamma_t=\frac{\lim_{x\to\infty}[x^{\nu+1}L(x)]}{\int_0^\infty[x^{\nu-1}L(x)dx]}. \tag{9}$$

γ_t can be calculated for three possible morphologies of the minority phase by simple geometric considerations. For the plate and spherical structures, γ_t can be calculated from [19]

$$\gamma_t=[\pi^2\phi(1-\phi)]^{-1} \tag{10}$$

and

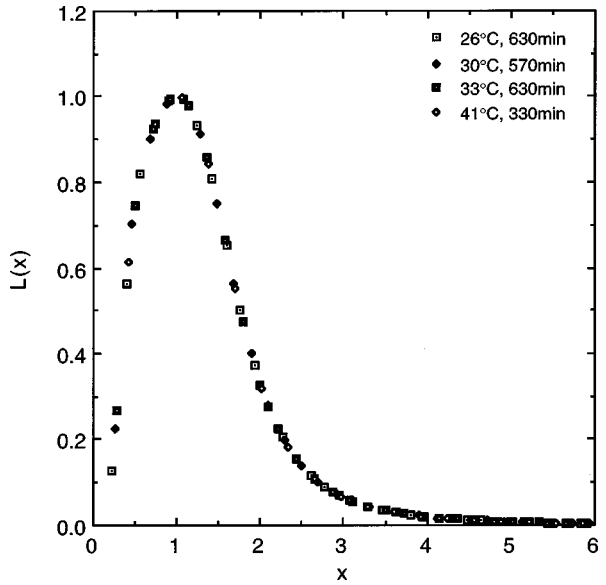

FIG. 6. Plots of the scaling function $L_3(x)$ versus $x=Q/Q_1$ at $\gamma=0.65$ for the 1:4 $C_{30}H_{62}/C_{36}D_{74}$ mixture quickly quenched from the melt to different temperatures 26, 30, 33, and 41 °C.

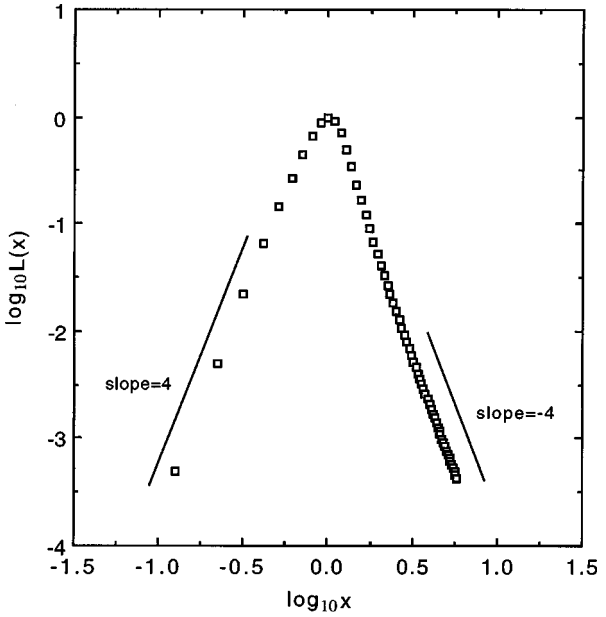

FIG. 7. A $\log_{10}$-$\log_{10}$ plot of $L_3(x)$ versus $x=Q/Q_1$ for the 1:1 $C_{30}H_{62}/C_{36}D_{74}$ mixture 570 min after quick quenching from the melt to 26 °C.

$$\gamma_t=\left[\left(\frac{2\pi^5}{9}\right)^{1/3}\phi^{1/3}(1-\phi)\right]^{-1}, \tag{11}$$

respectively. Figure 8 shows the volume fraction ϕ dependence of the theoretical and experimental values of γ. The volume fractions of the minority component in the C_{30}/C_{36} mixtures were calculated from unit cell axes of the pure paraffins [31]. The volume fractions of $C_{30}H_{62}$ in the $C_{30}H_{62}/C_{36}D_{74}$ mixtures are 0.460, 0.242, 0.175, and 0.086, respectively, corresponding to 1:1, 3:8, 1:4, and 1:9 $C_{30}H_{62}/C_{36}D_{74}$ mixtures. The volume fraction of $C_{36}D_{74}$ in 4:1 $C_{30}H_{62}/C_{36}D_{74}$ is 0.227. The volume fraction of $C_{30}D_{62}$ in 1:1 $C_{30}D_{62}/C_{36}H_{74}$ is 0.461, very close to the value for $C_{30}H_{62}$ in 1:1 $C_{30}H_{62}/C_{36}D_{74}$. The theoretical values γ_t are 0.58, 0.41, 0.54, 0.70, and 0.78 in terms of Eq. (10), corresponding, respectively, to 4:1, 1:1, 3:8, 1:4, and 1:9 $C_{30}H_{62}/C_{36}D_{74}$ mixtures. It is apparent that the theoretical values γ_t in terms of the plate structure are close to the experimental data but different from the experimental ones at low volume fractions in terms of the spherelike assumption. The results imply that the lateral dimension of lamellae in the minority phase is much smaller than the axial one.

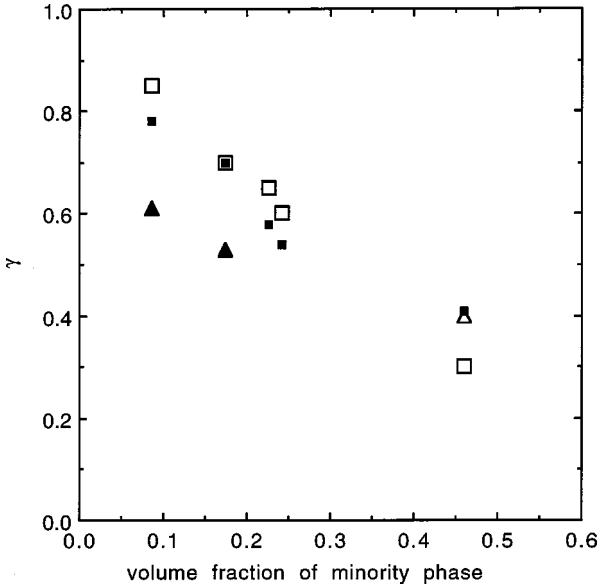

FIG. 8. Plots of the parameter γ versus volume fraction ϕ of the minority component in the mixtures. Empty and filled squares represent, respectively, the experimental and calculated γ values of the minority component in $C_{30}H_{62}/C_{36}D_{74}$ mixtures. The empty triangle is the γ value of the 1:1 $C_{30}D_{62}/C_{36}H_{74}$ mixture. The calculated values of γ were obtained in terms of Eq. (10). Filled triangles represent the calculated γ values of the 1:4 and 1:9 $C_{30}H_{62}/C_{36}D_{74}$ mixtures in terms of Eq. (11).

IV. CONCLUSION

In summary, the SANS experimental results indicate that the late stages of the microphase separation of paraffin mixtures are in good agreement with the universal features predicted by the FL scaling function. It has been demonstrated that, like alloys and polymer blends, the scaled structures of the paraffin mixtures depends on the volume fraction but not on the quench temperature. Porod's law of the scaling function $L(x)$ at large x and a dependence $L(x)\sim x^4$ at small x are observed, indicating a two-phase morphology and a domain growth of the Cahn-Hilliard mode. The theoretical values γ_t in terms of the plate structure assumption are found to be close to the experimental data, which allows the scaled structures of paraffin mixtures to be predicted from the volume fraction of the minority phase without any adjustable parameter.

[1] J. D. Gunton, M. S. Miguel, and P. S. Sahni, in *Phase Transitions and Critical Phenomena*, edited by C. Domb and J. L. Lebowitz (Academic, New York, 1983), Vol. 8.
[2] T. Hashimoto, Mater. Sci. Technol. **12**, 251 (1993).
[3] K. Binder, Adv. Polym. Sci. **112**, 181 (1994).
[4] P. DeBenedetti, *Metastable Liquids: Concepts and Principles* (Princeton University Press, Princeton, NJ, 1996), Chap. 3.
[5] R. G. Snyder, M. C. Goh, V. J. P. Srivatsavoy, and H. L. Strauss, J. Phys. Chem. **96**, 10 008 (1992), and references therein.
[6] D. Dorset, Macromolecules **23**, 623 (1990).
[7] J. W. White, P. W. Zhu, J. E. Epperson, D. Wozniak, and R. G. Snyder, Mol. Phys. **91**, 1017 (1997).
[8] J. W. White, P. W. Zhu, J. E. Epperson, and R. G. Snyder, Mol. Phys. **91**, 1039 (1997).
[9] J. W. White, P. W. Zhu, and J. E. Epperson, J. Phys. Chem. **100**, 19 967 (1996).
[10] J. Marro, J. L. Lebowitz, and M. H. Kalos, Phys. Rev. Lett. **43**, 282 (1979).
[11] M. K. Phani, J. L. Lebowitz, M. H. Kalos, and O. Penrose,

Phys. Rev. Lett. **45**, 366 (1980).
[12] H. Furukawa, Adv. Phys. **34**, 703 (1985).
[13] S. Komura and H. Furukawa, *Dynamics of Ordering Processes in Condensed Matter* (Plenum, New York, 1988).
[14] K. Binder, Mater. Sci. Technol. **5**, 405 (1991).
[15] M. Rao, M. H. Kalos, I. L. Lebowitz, and J. Marro, Phys. Rev. B **13**, 4328 (1976).
[16] T. M. Rogers and R. C. Desai, Phys. Rev. B **39**, 11 956 (1989).
[17] A. Chakrabarti, R. Toral, and J. D. Gunton, Phys. Rev. B **39**, 901 (1989).
[18] P. Fratzl and J. L. Lebowitz, Acta Metall. **37**, 3245 (1989).
[19] P. Fratzl, J. L. Lebowitz, O. Penrose, and J. Amar, Phys. Rev. B **44**, 4794 (1991).
[20] R. L. Pego, Proc. R. Soc. London, Ser. A **422**, 261 (1989).
[21] J. Cahn and J. Hilliard, J. Chem. Phys. **28**, 258 (1958).
[22] R. Snyder, V. J. P. Strivatsavoy, D. A. Cates, H. L. Strauss, J. W. White, and D. L. Dorset, J. Phys. Chem. **98**, 674 (1994).
[23] J. Marro, J. L. Lebowitz, and M. H. Kalos, Phys. Rev. Lett. **43**, 282 (1979).
[24] K. Binder and D. Stauff, Phys. Rev. Lett. **33**, 1006 (1974).
[25] K. Binder, Phys. Rev. B **15**, 4425 (1977).
[26] H. Furukawa, Phys. Rev. Lett. **43**, 136 (1979).
[27] D. Siggia, Phys. Rev. A **20**, 595 (1979).
[28] O. Glatter and O. Kratky, *Small Angle X-ray Scattering* (Academic, London, 1982).
[29] J. Martin and A. Hurd, J. Appl. Crystallogr. **20**, 61 (1987).
[30] F. Family and D. Landau, *Kinetics of Aggregation and Gelation* (North-Holland, Amsterdam, 1984).
[31] D. Dorset, Macromolecules **24**, 6521 (1991).